Contents lists available at ScienceDirect

Arabian Journal of Chemistry

journal homepage: www.ksu.edu.sa

Carboxymethyl cellulose/polyvinylpyrrolidone bio-composite hydrogels enriched with clove bud extracts for enhanced wound healing

Md. Monirul Islam, Md. Ibrahim H. Mondal *

Polymer and Textile Research Lab, Department of Applied Chemistry and Chemical Engineering, Rajshahi University, Rajshahi 6205, Bangladesh

ARTICLE INFO

Keywords:
Carboxymethyl cellulose
Polyvinylpyrrolidone
Clove extract
Antibacterial
Wound healing

ABSTRACT

In contrast to conventional chemical treatments, medicinal plants are more secure and efficient in treating wounds without the risk of adverse effects. Traditional wound dressings have no antibacterial features, and have an inadequate water vapour transmission rate (WVTR). Clove extracts (CE) were developed in this study to make the dressings more effective in humans. The morphological, physical, mechanical, biological, and antibacterial properties of CMC/PVP biocomposite films were explored with different clove extract (CE) concentrations (2 %, 4 %, and 6 %). Fourier transform infrared spectroscopy (FTIR) and X-ray diffraction (XRD) investigations demonstrated the structural relationships involving CMC, PVP, and CE in the reinforced samples. The TGA results validate the CMC/PVP/CE bio-composite hydrogel's potential for usage in medicinal applications. The developed bio-composite hydrogels showed > 87 % cell viability against Vero cells, were favourable to cell growth, and had a significant zone of inhibition against *S. aureus* and *E. coli* bacteria. CMC/PVP/CE (6 %) bio-composite hydrogel enhanced wound healing in albino mice within 12 days, had a WVTR of 2310 g/m^2-day and an ESR% of 1712 %. In addition, the results of the histological examination corroborated the observations of faster tissue regeneration, less inflammatory cells, and enhanced vascularity of the surrounding skin. The overall results encourage and show that CMC/PVP/CE (6 %) bio-composite hydrogels have a lot of potential uses in the biomedical field, especially for wound healing.

1. Introduction

The biggest organ in the integumentary system is the skin, which covers the entire body (Farazin et al., 2021). The prolonged healing process of chronic wounds makes it difficult to provide effective treatment (Wang et al., 2017; Mondal and Haque, 2019). Hydrogels are 3D networks that can retain varying amounts of water without dissolving. They are the consequence of physical and/or chemical crosslinking of macromolecules (Abdul Khalil et al., 2022; Mondal et al., 2022; Qamruzzaman et al., 2022). Because of their low toxicity and high absorption capacity for wound physiological exudates, hydrogels have found use in wound healing by creating a moisture balance that speeds up the healing process. Hydrogels' non-adhesiveness and smoothness are two major benefits that make it easy to remove them without harming wounds (El Fawal et al., 2018).

Biopolymers, such as chitosan, alginates, and starch, are used in hydrogel production, due to their distinctive characteristics. However, these natural materials possess limited mechanical strength and need additional modifications to match the performance of synthetic-based hydrogels (Abdul Khalil et al., 2022). Developing a functional encapsulating technology for medicinal extract use is the present obstacle. So, to broaden the scope of pharmaceutical uses, one option is to employ polymeric biomaterials like hydrogels (Zamora-Mendoza et al., 2023).

CMC, a polyanionic polymer, has been revealed to have bioadhesive properties, enabling it to adhere to the mucosal linings of the oral and digestive systems (Javanbakht and Shaabani, 2019). Since CMC is mucoadhesive, it enhances the absorption of medicines and decreases its degradation over time by prolonging its contact with the targeted tissues. Because of its high levels of biocompatibility, CMC affords an intriguing opportunity for wound healing and skin regeneration (Basu et al., 2018; Pornpitchanarong et al., 2022). PVP, a non-toxic and biocompatible polymer, has been employed in biomedical applications (Dai et al., 2012). Glycerin and garlic extract were previously governed utilising PVP as a matrix for complying antibacterial agents (Edikresnha et al., 2019). However, high humidity accelerates the degradation of PVP. Therefore, PVP is not suitable for use as a wound dressing in most places (Sriyanti et al., 2021).

The citric acid (CA) was used to crosslinked sodium

* Corresponding author.
E-mail address: mihmondal@gmail.com (Md.I.H. Mondal).

https://doi.org/10.1016/j.arabjc.2024.105945
Received 8 April 2024; Accepted 30 July 2024
Available online 31 July 2024

carboxymethylcellulose (Na-CMC) and hydroxypropylmethylcellulose (HPMC) hydrogel films (Dharmalingam and Anandalakshmi, 2019). However, CMC hydrogels have a very low mechanical strength, especially in swollen states, which restricts their use. Blending CMC with PVP solves this problem, expanding its potential to be a new type of wound dressing material (Yeasmin and Mondal, 2015). Antimicrobial performance tests and *in vivo* experiments were not used to evaluate the clinical efficacy of developed CMC/PVP films for wound healing applications [Chopra et al., 2022; Wang et al., 2007]. Boric acid, an antibacterial agent, was added to CMC/PVP hydrogel for burn or cut wound healing, although antioxidant and *in vivo* tests were not done [Saha et al., 2011].

Improper usage of antibiotics might lead to bacterial drug resistance (Deng et al., 2021). Antibacterial silver nanoparticles are commonly used in hydrogels, although they are expensive and biotoxic (Blacklow et al., 2019).

Recently, herbal medicine extracts, containing phytochemicals, have been explored for a potential cancer to prevent or treat cancer and for treating other diseases in humans because they are cost-effective and safe (Karimi et al., 2017).

Clove (*Syzigium aromaticum L.*, family *Myrtaceae*) is highly regarded as a powerful food preservative against spoilage by pathogenic germs (El-Maati et al., 2016). It is utilised in medicine to slow aging, for wound healing and for treatment of thyroid dysfunction, skin cancer, digestive problems, and cardiovascular diseases. Cloves have bioactive phenolic compounds that possess anti-oxidant, anti-viral, anti-bacterial, and anti-cancer effects. Cloves are a prominent natural antioxidant in food products because of their high level of bioactivity (Ahmed et al., 2022).

Its main medicinal components are eugenol, eugenol acetate, and β-caryophyllene. Clove oil is GRAS (Generally Regarded As Safe), according to the FDA (Hameed et al., 2021). Eugenol has antioxidant, carminative, antispasmodic, antiseptic and antibacterial properties. It also demonstrates antimutagenic effects (Karimi et al., 2017).

Reduced porosity, limited antimicrobial activity, difficulties in discarding the dressing after healing, and allergic reactions have been identified as shortcomings in wound dressings in recent years. CMC/PVP hydrogels, comprising CE, have not yet been developed. Therefore, this research focuses on both *in vitro* and *in vivo* evaluation of prepared CE-impregnated antibacterial CMC/PVP bio-composite hydrogels for wound healing applications.

2. Experimental

2.1. Materials

Sodium Carboxymethyl Cellulose (Na-CMC, average $M_w \sim 250{,}000$, degree of substitution 0.9), Polyvinyl pyrrolidone (PVP, average $M_w \sim 29{,}000$), 100 % ethanol, and citric acid were purchased from Merck (Germany). Tween 80 and Folin – Ciocalteu reagents were purchased from Loba (India). Gallic acid and quercetin were procured from SRL in India. Aluminium chloride and sodium acetate were acquired from Merck in Germany. DPPH was purchased from Sigma-Aldrich (Germany) and nebanol ointment was purchased from Square Pharma (Bangladesh). Clove buds were purchased from Organic™ company, Bangladesh. All the compounds were of analytical grade and were utilised without any further purification.

2.2. Process for the preparation of clove extract (CE)

Dried clove buds were collected from a local market at Rajshahi, Bangladesh for extraction. They were dried at 40 °C for 8 h in an oven before being processed to a fine powder in a mill. The dried materials were ground in a mixer and stored as a powder (moisture content: 4 % dry basis). The resulting powder (10 g) was extracted with 1:1 water and ethanol for 72 h using a Soxhlet apparatus (1000 mL). After that, the sample was centrifuged at 8500 rpm for 10 min. The supernatant liquid was concentrated using a rotary evaporator at 35 °C for solvent removal, then lyophilized and, finally, dissolved in 2 % Tween 80 solution, ensuring the concentration of 1 mg/mL for further uses (Tayel et al., 2020; George et al., 2020; Mittal et al., 2020; Mondal and Saha, 2019).

2.3. Determination of total phenolic content

The Folin—Ciocalteu method was employed to ascertain the total phenolic content of the clove extract. A solution containing 1 mL of extract, with a concentration ranging from 10 to 500 μg/mL, was combined with 5 mL of 10 % (w/v) Folin—Ciocalteu reagent. 5.0 mL of 7.5 % (w/v) Na_2CO_3 was added to the mixture after 5 min and it was then incubated, at 25 °C, for an hour. Subsequently, absorbance was measured, using a UV Spectrophotometer (Shimazu, UV-1800), at a wavelength of 765 nm against the blank. The results were expressed in milligrams as gallic acid equivalents per gram of dry extract (mg GAE/g) (Aryal et al., 2019).

2.4. Determination of total flavonoids content

The flavonoid content of clove extract was measured using the Dowd method. 1 mL of clove extract solution (10–500 μg/mL) or quercetin (10–500 μg/mL) was combined with 200 μL of 10 % (w/v) $AlCl_3$ solution in 3 mL methanol, 200 μL (1 M) potassium acetate and 5.6 mL distilled water. The mixture was incubated for 30 min at room temperature, followed by the measurement of absorbance, at 415 nm, against the blank. The results were expressed as milligrams of quercetin equivalent (QE) per gram of dry extract (Aryal et al., 2019).

2.5. Preparation of CMC/PVP/CE bio-composite

The hydrogel films were developed by the solution-casting method, utilising an aqueous solution, comprised of Na-CMC, PVP, and citric acid, as a cross-linker. A 5 % (w/v) Na-CMC solution was prepared by dissolving 1 g Na-CMC in 20 ml deionized water and thermally treating it with citric acid (10 % based on the total polymer matrix) at 165 °C, in a hot-air oven, to attain CA crosslinking of Na-CMC. A 5 % (w/v) PVP solution was prepared and mixed with a CA-crosslinked CMC solution at a constant ratio of 4:1 (v/v), to obtain CMC/PVP blends (Roy et al., 2012). The blending process took place at 80 °C for 60 min with gentle stirring. To make the bio-composites, a mixture of CA- crosslinked CMC and PVP was prepared. Then the mixture was gradually added to a CE suspension of the solution (dissolved in Tween 80), with varying concentrations of CE (2 %, 4 %, and 6 % wt%), while continuing to agitate the mixture. After adding 0.25 mL sorbitol (per gram of polymeric mixture) as a plasticiser, the mixture was sonicated using a digital ultrasonic cleaner (YJ5120-1), for 15 min, at 25 °C. The solution was then put in a petri dish and left for 24 h for air drying. After that, it was taken to the freeze-dryer (Huang et al., 2023).

2.6. Physical characterisation

The thickness of the prepared composites was measured with a digitally-calibrated micrometer (Digipa, Mitutoyo, Japan). At least ten locations across each film were measured to get an average thickness. Both the mean and the standard deviation were provided (Chopra et al., 2022).

Five random samples ($n = 5$) (1×1 cm^2) were taken to assess the films' weight consistency, and the weight of each sample was measured separately, using an electronic weighing balance (Rashid et al., 2023). The folding endurance was assessed to determine how many times the film could be folded. The folding endurance value was determined by counting the number of times a film sample could be folded in the same place without breaking. The test was carried out in triplicate (Mohammadi et al., 2018).

2.7. Attenuated total Reflectance (ATR)–Fourier transform infrared (FTIR) analysis

ATR-FTIR spectroscopy was carried out to analyse the CMC/PVP hydrogel and CMC/PVP/CE biocomposite. The *spectra* were recorded in a range between 4000 cm^{-1} and 400 cm^{-1}, using a Perkin Elmer FTIR spectrophotometer (Model: Paragon 500, Perkin Elmer, UK), with a smart orbit Attenuated Total Reflectance (ATR) accessory. The ATR is fitted with diamond crystal. The ATR-FTIR spectrum was taken in a transmittance mode (Gholamali and Yadollahi, 2020).

2.8. X-ray diffraction

To determine phase identification and the crystalline nature of prepared hydrogel membranes, XRD analysis was conducted. It was performed using a PAN Analytical X Pert PRO X-ray diffractometer (Rigaku, Smart Lab, Japan). Crystallinity was evaluated using Cu-K radiation at a wavelength of 1.5406 on CMC, PVP, CMC/PVP, and CMC/PVP/CE biocomposites. The scanning rate was 2 min over a period with a scanning angle from 5° to 70° (Altaf et al., 2021).

2.9. Thermogravimetric analysis (TGA)

The thermal degradation behaviour of the films was investigated by a Pyris TGA linked to a Pyris diamond TA Lab System (Perkin-Elmer Co., USA). Measurements were performed on 10–15 mg samples in an aluminum pan under an inert N_2 atmosphere with a flow rate of 50 mL/min in a temperature range from 40 to 500 °C with a heating rate of 10 °C/min. The weight loss and its first derivative were recorded simultaneously as a function of time/temperature (Fiorentini et al., 2021).

2.10. Field emission scanning electron microscopy (FESEM)

When working with electrons, rather than light, an electron microscope is referred to as an FESEM. A field source of emission releases these electrons. Using FESEM (JEOL, Model- JSM7600 F, Japan), the surface morphology of the produced samples of CMC, PVP, CMC/PVP hydrogel, and of the CMC/PVP/CE biocomposites were examined. The scans were carried out at 5.0 kV accelerating voltage and the FESEM images were captured using the ultra-high resolution electron imaging mode (Gupta et al., 2020).

2.11. Determination of swelling propensity

0.1 g of dry sample (1 × 2 cm^2, thickness 0.3 mm) was immersed in water and periodically removed. Surface water was absorbed by dabbing with a filter paper. Swollen hydrogels were weighed, and the percentage of water absorption capacity was measured by the following equation.

$$S\,(\%) = \frac{M_s - M_d}{M_d} \times 100 \quad (1)$$

where S is the equilibrium water absorbency (%), M_s and M_d are the weight of swollen hydrogel (g) in three different solutions – distilled H_2O of pH 7, phosphate buffer i.e blood of pH 7.4 and simulated gastric fluid i.e HCl buffer of pH 1.2 – respectively (Chopra et al., 2022).

2.12. Water vapour Transmission, moisture retention capability and porosity test

The water vapour transmission rate (WVTR) was calculated using the European Pharmacopoeia (EP) standard. Hydrogel film samples (0.1 g, 1 × 2 cm^2, thickness 0.3 mm) were cut into circular pieces and taped to the mouth of a 35 mm-inner-diameter container, containing 25 mL distilled water. The bottles were then kept in an oven at 35 °C, with a relative humidity of 35 %. The formula used to calculate the WVTR (g/m^2-day) is given below:

$$\text{Water Vapour Transmission Rate} = \frac{W_i - W_f}{A} \times 10^6 \quad (2)$$

where A is the permeation area of samples, and Wi and W_f are the initial and final weight of bottles, respectively. The experiment was conducted at 35 °C as the end application of the hydrogel on human skin, which had a temperature of 37.2 °C (Khorasani et al., 2018).

The capability of the prepared hydrogel membranes to retain water was determined. The samples were placed in an oven, at 40 °C, for 6 h and weighed. The ability to retain moisture was calculated using Equation (3):

$$\text{Moisture Retention Capability} = \frac{W_1 - W_2}{W_1} \times 100 \quad (3)$$

where W_1 is the initial weight and W_2 is the weight in grams after 6 h of heating at 40 °C.

The experiment was conducted at 40 °C, beyond the human body temperature of 37.2 °C, to align with the practical application of our findings on human skin. The temperature was maintained within ranges of the water vapor transmission rate and moisture retention capability in both situations (Altaf et al., 2021).

Porosity is a measure of empty spaces in a material that is expressed as a fraction of the volume of such empty spaces over the total volume of the material, ranging from 0 to 1, or as a percentage between 0 % to 100 %. The porosity of the bio-composite hydrogels was determined using the alcohol displacement method. In brief, the initial weight and volume (W and V) of the lyophilised gels were measured and recorded. The gels were then immersed in dehydrated alcohol until completely saturated. The gels were weighed again after the surface liquid was removed. The porosities were calculated using the following equation:

$$P\,(\%) = (W_2 - W_1)/\rho\, V_1 \quad (4)$$

where W_1 and W_2 indicate the weight of the bio-composite films before and after immersion, respectively, V_1 is the volume before immersion and ρ is the density of alcohol at room temperature (Yuan et al., 2021).

2.13. Polyphenol drug release studies

At 45 °C, a bio-composite hydrogel sample of 0.1 g CMC/PVP/CE (6 %) was dried. After that, it was submerged in 25 mL of pH 7.4 PBS. Using a vibrator (HY-4C Cycling Vibrator) set to 25 rpm for 72 h at 37 °C, the experiment was conducted. The sample's highest peak was observed at 280 nm, according to the UV/Vis profile of the extracts. The linear regression equation that corresponds to the Korsmeyer-Peppas math model was used to fit the absorbance value that corresponds to the release profiles. This model is based on the CE released from the developed bio-composite hydrogel (Pramod et al., 2013; Zamora-Mendoza et al., 2023).

2.14. Biological evaluation

In an agar-nutrient medium, the microorganisms *Escherichia coli* and *Staphylococcus aureus* were cultured. The prepared films were then cut into a circle with a diameter of about 6 cm. After culturing the bacteria, the cut film pieces were placed on the culture surface. After 48 h of storage at 37°C, the circular area of the inhibited zone around the film was measured 3 times and the average of these measurements was recorded (Hosseini et al., 2021; Saha et al., 2023). The 2,2-diphenyl-1-picrylhydrazyl (DPPH) radical was used to examine the antioxidant activity of CMC-based composite films. The film sample, weighing approximately 50 mg, was submerged in 5 mL of a 0.004 % (w/v) DPPH methanol solution and left to incubate, at room temperature, for 60 min. Then the sample was tested, with a UV–vis spectrophotometer, and its absorbance was found to be greatest at 517 nm. For comparison, the same DPPH solution was utilised without the film. The extent of antioxidant activity in film samples was measured (Arrua et al., 2010) as

follows:

$$\text{Free Radical Scavenging Activity}\,(\%) = \frac{(A_c - A_s)}{A_c} \times 100 \quad (6)$$

where Ac and As were the absorbances of DPPH of the control and the test film, respectively.

2.15. Cell viability test and hemolytic potentiality test

Cell viability was determined employing Vero cells, which are derived from the kidney cells of African green monkeys, to examine the composite films. Samples with a diameter of 16 mm were punched from the dry composite films. After 10 min in an autoclave, at 121 °C, the samples were transferred to 24-well culture plates and sterilised. Each well was given 1 mL of minimal essential medium (MEM) culture media, supplemented with 10 % fetal calf serum, and left there for 30 min, to acclimate with the samples. Each well was equipped with a metal ring and 0.5 mL of MEM culture media, supplemented with 10 % fetal calf serum, before cell seeding. Both the composites' film, and the control, were planted, at a density of 6×10^4 cells per well, in 24-well culture plates. The cells were kept at 37 °C, in a 5 % CO_2 humidified incubator, for 16 h. After 48 h, the medium was changed to MEM without serum, to continue growing the Vero cells. An MTT (3-[4,5-dimethylthiazol-2-yl]-2,5 diphenyl tetrazolium bromide) assay was used to determine the number of live cells at the end of the incubation (Taokaew et al., 2013). Hemolysis takes place when an erythrocyte membrane ruptures and releases haemoglobin into the bloodstream. Hydrogels, comprised of CMC/PVP and CE, were investigated for their hemolytic activity. The blood-testing solution was prepared by mixing 2.5 mL of 0.9 % saline with trisodium citrate, a blood anticoagulant. The film segments (20 mg, roughly 1 cm × 1 cm) were pre-incubated in 4 mL of saline for 30 min, at 37 °C, before being incubated in 0.1 mL of diluted blood, for 60 min, at 37 °C. Positive and negative control samples were tested, using 0.1 mL of diluted blood and 4.0 mL of distilled water (100 % hemolysis) or saline solution (0 % hemolysis). All solutions were centrifuged for 5 min at 1500 rpm. After measuring the supernatant's absorbance at 545 nm, the hemolysis was estimated as follows:

$$\text{Hemolysis}\,(\%) = \frac{(OD_{sam} - OD_{neg})}{(OD_{pos} - OD_{neg})} \times 100 \quad (7)$$

here, where ODsam, ODneg, and ODpos are the adsorptions of the sample, negative control, and positive control, respectively (Lu et al., 2017).

2.16. In vivo wound healing study

To further evaluate the potential of hydrogel dressings in the field of wound healing, mice full thickness skin defect repair tests were conducted. Male albino mice, that weighed around 50 grammes each, were used as test subjects. The albino mice were anesthetized and shaved. Then they were cut to produce a full-thickness skin wound of 10 mm in diameter. The mice were divided into five groups, each group being given a different dressing: nebanol (an antibiotic); CMC/PVP; or CMC/PVP/CE (6 %) were used to treat the wounds right away. Three rats (n = 3) were placed in each group, and they were free to eat and drink as they pleased (Abdollahi et al., 2021). The wound healing (%) was determined by the following equation-.

$$\text{Wound healing}\,(\%) = \frac{A_0 - A_t}{A_0} \times 100 \quad (8)$$

where A_t and A_0 were the wound areas on the testing day and the wounding day, respectively. These calculations validated the advantages of hydrogels as wound dressings.

For histological images, on the 12th day, the mice were killed. The wound tissue samples were thoroughly biopsied/ Then the tissue samples were fixed in a 10 % neutral buffered formalin for 24 h, embedded in paraffin, and sliced at a thickness of 6–10 μm, using a microtome. The sections were deparaffinized, dehydrated through a series of graded ethanol, stained with hematoxylin and eosin (H & E), and viewed using an optical microscope (OLYMPUS, CX31, Tokyo, Japan) (Kim et al., 2016; Jakfar et al., 2022).

2.17. Statistical analysis

All the experiments were conducted in triplicate and the data are presented as mean values ± standard deviation. The resultant zones of inhibition for the antibacterial activity of the samples around the discs were measured in mm.

3. Result and discussion

3.1. Clove extract %, total phenolic and flavonoid content

The percentage yield of clove extract was 17.5 ± 0.25. Total phenolics (TPC) and flavonoids (TFC) were estimated in the extracts using colorimetric assays. TPC of the clove extract was calculated from the regression equation of calibration curve ($y = 0.0009x + 0.0295$, $R^2 = 0.9967$) and expressed as mg gallic acid equivalents (GAE) per gram of extract (mg/g). The phenolic content of clove in water using ethanol (1:1) extract was estimated to be 207.22 ± 0.26 mg GAE/g.

Total Flavonoids content of the extracts was calculated from the regression equation of calibration ($y = 0.0015x + 0.0447$, $R^2 = 0.9969$) and expressed as mg quercetin equivalent (QE) per gram extract (mg/g). The flavonoid content was 351.53 ± 0.05 mg QE/g (Adaramola and Onigbinde 2016).

3.2. Physical evaluation of the prepared films

The addition of CE to CMC/PVP increases the weight and thickness of the films, affecting their structural integrity significantly. Table 1 shows the thickness and weight variation of films prepared with the three CE concentrations, as well as of films prepared without CE. The thicknesses of the CMC/PVP-loaded CE films were found to be higher than those of the CMC films without CE (Control). The increase in CE content in the CMC/PVP film from 0 % to 6 % resulted in an increase in thickness from 0.206 mm to 0.265 mm and weight from 0.021 g to 0.027 g. The upward trend in thickness values could be the result of the higher solid content and structure of the manufactured CMC/PVP/CE films (Anwar et al., 2022).

The folding endurance of composite films, meaning their capacity to withstand any rupture, ranged from 102 to 134. Because of the intermolecular forces between the CMC/PVP polymeric chain and CE, folding endurance was greater in bio-composite hydrogels with a higher CE content, as shown in Table 1. However, the presence of slight differences in the arrangement of CE in the core and peripheral areas led to a significant revelation of variances in both thickness and weight.

3.3. ATR-FTIR analysis

The FT-IR *spectra* of CMC, PVP, citric acid, biogenic CE, MC/PVP and the CMC/PVP incorporated with CE, in the wavelength range of

Table 1
Thickness, weight variation and folding endurance of the prepared CMC/PVP film (control) and CMC/PVP/CE films.

Film Samples	Thickness (mm)	Weight (g)	Folding Endurance
CMC/PVP (Control)	0.206 ± 0.028	0.021 ± 0.001	102 ± 4
CMC/PVP/CE (2 %)	0.221 ± 0.027	0.023 ± 0.003	114 ± 3
CMC/PVP/CE (4 %)	0.245 ± 0.026	0.025 ± 0.002	126 ± 5
CMC/PVP/CE (6 %)	0.265 ± 0.022	0.027 ± 0.003	134 ± 2

*Data are expressed as mean ± standard error of three replicates.

400–4000 cm^{-1} are shown in Fig. 1. Peaks between 3300 cm^{-1} and 3500 cm^{-1} wave numbers, for all samples, are produced by hydroxyl groups (–OH), which imply that the hydrogel has hydrophilic properties and thus can absorb excess water in wounds. Peaks between 2800 cm^{-1} and 3000 cm^{-1} wave numbers, for all samples, are attributable to C–H stretching vibrations. The absorption peaks of CMC appear at 1418 cm^{-1}, indicating the presence of $–CH_2–$ groups. The peaks at 1602 cm^{-1} indicate the presence of a carboxyl group (COO^-) and more intense vibrations at 1032 cm^{-1} indicate the presence of ether linkage (C–O-C). Some characteristic peaks in the PVP *spectrum* could be assigned as follows: 1284 cm^{-1} to C–N stretching vibration; 1431 cm^{-1} to $–CH_2–$ wagging; 1644 cm^{-1} to C=O stretching vibration. In citric acid, peaks at 1105 cm^{-1} can be assigned to C-O stretching, and at 1721 cm^{-1}, to C=O stretching. In CE, at 1729 cm^{-1}, looking at the frequency pattern for the ester group of C-O, the peak at 1618 cm^{-1} belongs to the aliphetic alkenes and the one at 1520 cm^{-1}, stretching of the aromatic moiety. The peak at 1043 cm^{-1} is attributable to C-O stretching.

Looking at results for the CMC/PVP hydrogel, there was a new peak at 1740 cm^{-1}, indicating ester linkage with CMC by CA. The new peak at 1274 cm^{-1} is attributable to C–N stretching, due to the crosslinking of PVP with CMC. CMC/PVP/CE (6 %) also showed ester linkage at 1740 cm^{-1}, while new peaks, at 1618 and 1520 cm^{-1}, confirm the presence of eugenol in CE of the the developed bio-composite (Mondal et al., 2015; Alghunaim, 2019; Ramadoss et al. 2019; Pramod et al., 2015; Parthipan et al., 2021).

3.4. X-ray diffraction (XRD)

In the XRD of CMC, as shown in Fig. 2**a,** the peak at 22.6°, with lower intensity, indicates a decrease in the crystallinity of the substance because of cleavage of the hydrogen bonds among cellulose molecules. This cleavage is the result of the alkalisation of cellulose. Characteristic peaks are found at $2\theta = 11.2°$ and 20.4°, attributable to PVP. The presence of a broad peak at 22.8°, with some small peaks (6.2°, 10.8°,12.5°, 27.4°) confirms the presence of CE in the CMC/PVP bio-composite hydrogels. These results show that the CE and the CMC/PVP composite have bonded, consistent with the FTIR result.

3.5. Thermogravimetric analysis (TGA)

Thermal stability at a temperature range of 30–150 °C is very crucial for polymeric materials for medical applications (George et al., 2020). From the TGA curves depicted in Fig. 2**b**, there was an initial weight loss for all three cases up to 100 °C and this could be attributed to the release of surface moisture from the samples. In CMC, the major decomposition started at 232 °C, with due to inorganic moiety. Moreover, the decomposition after 354 °C occurred due to the pyrolysis reaction. The CMC/PVP blend was found to be relatively stable and its decomposition temperature was above 254 °C. But the thermal stability of CMC/PVP/CE (6 %) was relatively low and its decomposition temperature is below 232 °C due to its lower crystallinity as compared to CMC and CMC/PVP blend. It is also supported by the XRD result. It is clear that up to 30–150 °C, around 78 % weight of the CMC/PVP/CE (6 %) sustained confirms that the CMC/PVP/CE (6 %) bio-composite is a good carrier and suitable for medical applications.

3.6. Field emission scanning electron microscopy (FESEM)

Field emission scanning electron microscopy was used to examine the shape and size of the prepared materials. The surface morphologies of CMC, PVP and hydrogel, both with and without CE addition, were analysed by FESEM and the results are shown in Fig. 3. CMC shows a crystalline and needle-like structure and PVP shows a globular structure. But CMC/PVP hydrogel shows a homogeneous blended structure, which confirms successful crosslinking among the constituents of the bio-composite hydrogels. FESEM images of the cross-section of the CMC/PVP/CE composite film revealed that there were no voids in the bio-composite films and that the nanofillers CE were distributed evenly in the polymer matrix without aggregation. This indicates that the fillers are consistent with the polymer matrix and have potentially good

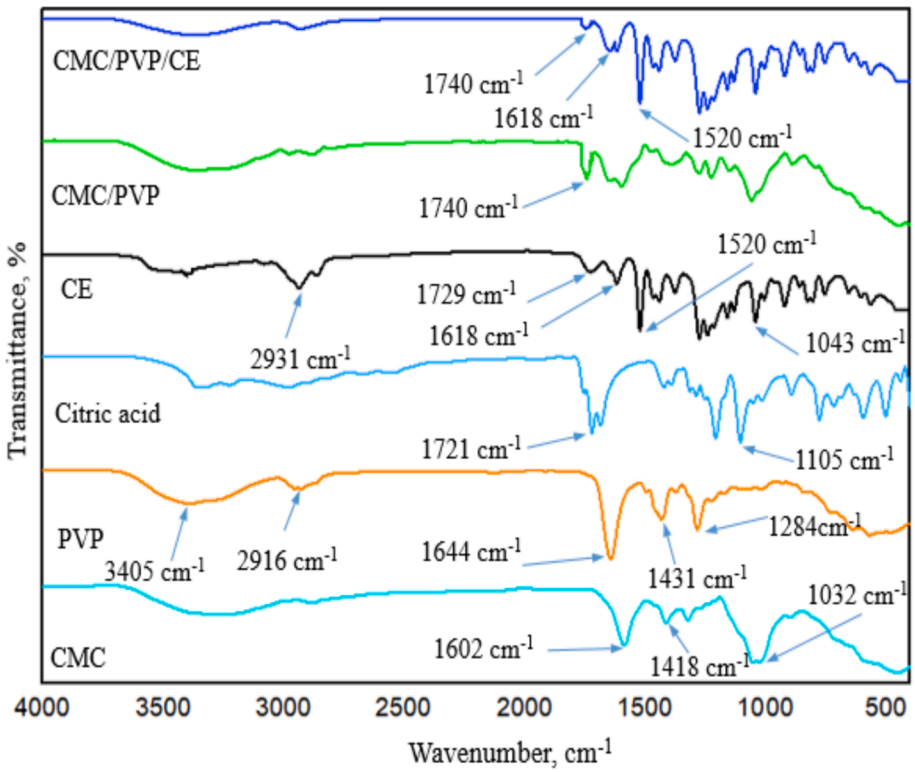

Fig. 1. FTIR spectra of CMC, PVP, citric acid, CE, CMC/PVP hydrogel and CMC/PVP/CE (6%) bio-composite hydrogel.

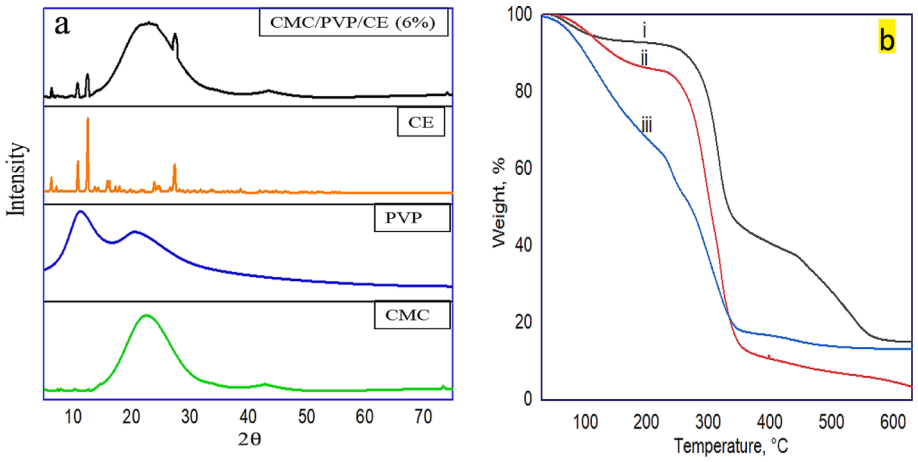

Fig. 2. (a) XRD patterns of CMC, PVP, CE, and CMC/PVP/CE (6%), and (b) TGA curves of the prepared samples i. CMC/PVP, ii. CMC, and iii. CMC/PVP/CE (6%).

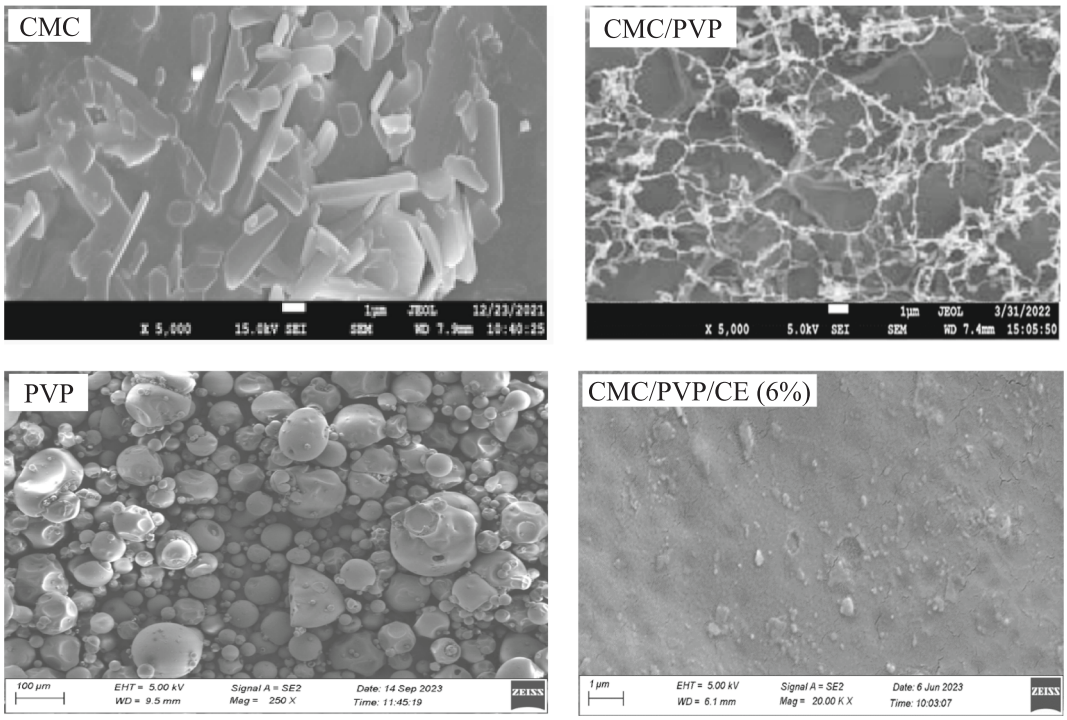

Fig. 3. FESEM images of CMC, PVP, CMC/PVP, CMC/PVP/CE (6%) samples.

adhesion, intermolecular binding, and affinity. The hydrogels including CE exhibited a transformation in morphology, resulting in the formation of porous structures of varying sizes and shapes. Incorporating CE into the hydrogel also resulted in a crystalline, fibre-like structure that was similar to CMC. Rapid evaporation of the extract's eugenol oil is represented by the creation of macro voids. Antimicrobial testing also confirms these findings. The FESEM also shows that the extract's insoluble particles are visible. However, because to their inimiscibility in water, cloves begin to produce pores as the addition of extract begins. This is because polar solvents are not well-suited to compounds with a high concentration of phenolic groups, as the hydroxyl groups become less effective (Altaf et al., 2021).

3.7. Swelling capacity

The swelling capacity of a hydrogel membrane plays a vital role in antibacterial activity, wound healing capacity, and biomedical applications, due to its water-holding capacity. The hydrogel membranes can absorb significant quantity of wound exudate by swelling, resulting in more-rapid wound healing (Baghaie et al., 2017). The water uptake of the films was tested in three solutions: phosphate buffers of pH 7.4 and 6.8 and stimulated gastric fluid (i.e. HCl buffer of pH 1.2), as shown in Fig. 4, to investigate the pH sensitivity of hydrogels. Increased water intake was observed in all samples at pH levels, meaning those above pH 7.4. At pH values higher than the pKa of carboxylic groups (pKa 4–5), the carboxylic acid groups become deprotonated, and increased electrostatic repulsion among the carboxylate ions expands the hydrogel matrix, allowing more water to penetrate it: i.e enhanced swelling (Altaf et al., 2021; Pourjavadi et al., 2006).

Most carboxylate anions are protonated at low pH levels. The network decreases when the electrostatic repulsion between carboxylate groups is decreased, leading to lower water absorption levels. Presumably, the hydrogen bonding between the carboxylate groups leads to polymer–polymer interactions and predominates over the

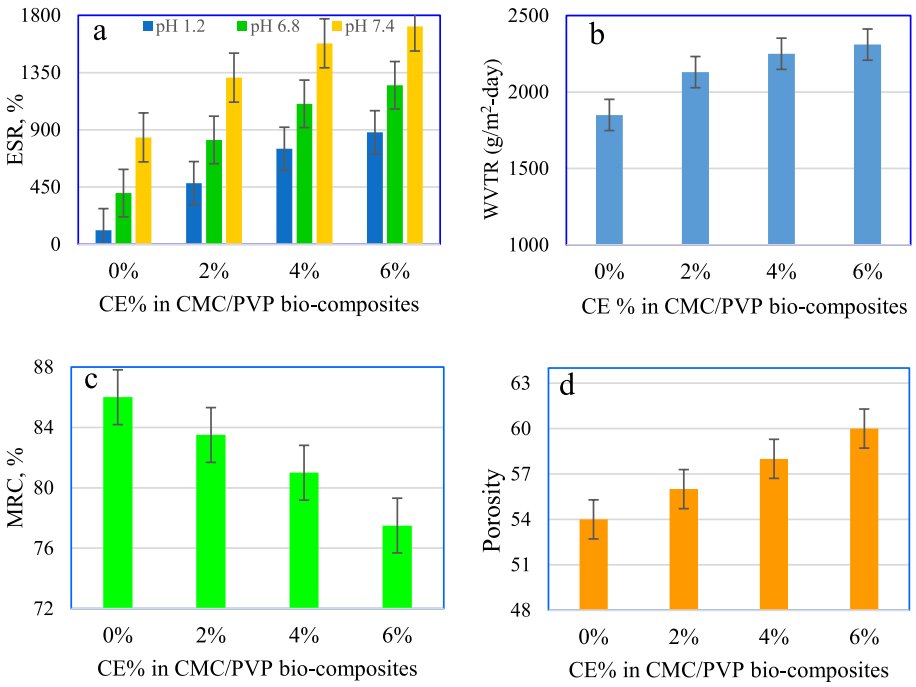

Fig. 4. Effect of %CE on (a) ESR, (b) WVTR, (c) MRC and (d) porosity of the prepared CMC/PV/CE bio-composite hydrogels.

polymer–water interactions. Hence, the electrostatic repulsion among these groups decreases and shrinkage occurs. Consequently, the swelling ratio is lower. However, at higher pH, the carboxylate groups tend to ionise and give off COO^- ions, which facilitate swelling. Furthermore, electrostatic repulsion between carboxylate ions should cause a macromolecular chain relaxation and increase swelling (Bialik-Wąs et al. 2021; Haque and Mondal, 2016) As shown in Fig. 4. the CMC/PVP film exhibits the least swelling, 840 %, at pH 7.4, due to the presence of strong hydrogen bonding between the biopolymers of CMC and PVP. This interaction allows water absorption and swelling without dissolution.

Fig. 4**a** shows that addition of CE to the CMC/PVP hydrogel increases the water absorption compared to CMC/PVP alone, due to the greater affinity of water for phytochemicals. The presence of CE is believed to disrupt the polymer networks and enhance the free volume of the CMC/PVP polymer blend. This results in heightened local segmental motions of the polymer, increased chain mobility, and ultimately, an augmentation in the water absorption capacity of the sample. Furthermore, carboxymethyl cellulose (CE) possesses a notable water absorption capability in its own right. Therefore, incorporating this material into the CMC/PVP composite hydrogel could alone enhance the hydrophilic nature of the sample. Moreover, the porosity of the hydrogels increased with the addition of 6 % CE, leading to an expansion in swelling capacity, as observed using FESEM analysis.

The swelling capacity of the prepared bio-composite hydrogels increases with increasing concentrations of CE upto 6 % and pH values. CMC/PVP/CE (6 %) film exhibits the highest swelling of 1712 %, at pH 7.4 (Mittal et al., 2020; Wang et al., 2020; Alvandi et al., 2023; Ali et al., 2023).

3.8. *Water vapour transmission rate and moisture retention capability*

Keeping the wound's surface moist is an essential requirement for an ideal wound dressing. The potential of hydrogel dressings to keep wounds moist is shown in the transfer of body fluids or wound exudates with the rate of water vapour transfer (WVTR). Such transfers directly regulate ambient humidity for proper wound healing. Reduction of the WVTR leads to the accumulation of wound exudate and infection, delays the healing process, and increases the risk of bacterial growth. On the other hand, a higher value of WVTR facilitates faster drying and leads to more scar formation. The ideal wound dressing should have a WVTR of 2000–2500 g/m^2-day (Ali et al., 2023; Jangde et al., 2018).

Fig. 4**b** shows the WVTR of the prepared hydrogels over 24 h. The Figure shows that WVTR increases with the addition of CE content to CMC/PVP hydrogel. The significant increase in WVTR may be due to the greater porosity of the CMC/PVP/CE compared to the CMC/PVP hydrogel, as depicted in the FESEM images and the swelling results. The high porosity of the hydrogel facilitates the penetration and transfer of water vapour through it. The lowest WVTR value were observed for CMC/PVP is 1850 g/m^2-day. The WVTR values were 2130 g/m^2-day for CMC/PVP/CE (2 %), 2250 g/m^2-day for CMC/PVP/CE (4 %), and 2310 g/m^2-day for CMC/PVP/CE (6 %) bio-composite hydrogels (Ali et al., 2023; Stanicka et al., 2021).

The ability to retain moisture within the hydrogel matrix is referred to as moisture retention capacity. The presence of moisture promotes skin health and tissue regeneration. Therefore, hydrogel wound dressings with a high capacity for moisture retention are preferable. Fig. 4**c** shows the film's ability to retain water after 24 h of air exposure a room temperature, at various CE content levels. CMC/PVP with 0 % CE has the highest 86 % moisture retention capability. As the CE content increased, the film's capacity to adhere to moisture decreased significantly. The lowest MRC, i.e. 77.5 %, was for CMC/PVP/CE (6 %), due to its having the highest WVTR as also approved by the FESEM result. The results showed that CE is the best candidate for wound dressing applications. But, with the increase in concentration of CE, the value of MRC decreased. This is ascribed to the dominance of phenolic groups present in it (Altaf et al., 2021).

The porosity of the CMC/PVP composite hydrogel is 54 %. The high porosity of hydrogels incorporating CE is shown in Fig. 4**d**. The porosity is enhanced as the concentration of CE in the hydrogel membrane is increased. Porosity in the range 30–40 % is considered good for wound healing. The porosity of the membrane is highly dependent on the moisture retention capability of the bio-composite hydrogel membrane. FESEM images also show that the presence of CE in the bio-composite hydrogel enhances porosity, as CMC/PVP/CE (6 %) showed 60 % porosity. However, with the addition of CE, porosity decreased as like as

WVTR and ESR (Altaf et al., 2021).

3.9. Bioactive CE release study

The experimental result of the *in vitro* extract released from CMC/PVP/CE (6 %) in PBS at a pH of 7.4 is shown in Fig. 5. After fitting experimental data to the Korsmeyer-Peppas model, it was determined that the increased extract amount released is proportional to the bio-composite hydrogel weight. The extract release occurred owing to the pore size increase in the matrix network due to swelling of CE loaded CMC/PVP bio-composite hydrogel. Fig. 5 indicates that CMC/PVP/CE (6 %) bio-composite hydrogel demonstrated a CE extract releasing up to 80 %.

3.10. Biological evaluation

The antibacterial efficacy of the CMC/PVP, CMC/PVP/CE (2 %, 4 %, 6 %), and antibiotic (positive control) formulations was assessed by testing them against two types of bacteria: the gram-negative strain, *Escherichia coli* (*E. coli*), and the gram-positive strain, *Staphylococcus aureus* (*S. aureus*). The results are presented in Fig. 6**a and b**. They indicate that the zone of inhibition (ZoI) measurements varied for different samples against *S. aureus* and *E. coli* after the incubation period. The ZoI values were observed to be 6 mm, 14 mm, 20 mm, and 25 mm and 29 mm for *S. aureus*, and 6 mm, 11 mm, 13 mm, 18 mm, and 23 mm for *E. coli*. These results show the antibacterial properties of the bio-composite hydrogels containing CE. The correlation between CE and antibacterial efficacy is especially strong because, uniformly, the size of the Zone of Inhibition (ZoI) increases as the concentration of CE increases. The test also suggests that the hydrogels exhibited greater efficacy against *S. aureus* than against *E. coli*. This difference can be explained by the fact that the thick peptidoglycan layer of *S. aureus* bacteria facilitates the penetration of antibacterial agents, whereas the thin peptidoglycan network of *E. coli* is shielded by its lipopolysaccharides (LPS) layer. Whether or not this means that the hydrogel is more effective against gram-positive bacteria than gram-negative bacteria generally merits further investigation.

Observation of all the prepared bio-composite films indicates that the CMC/PVP/CE (6 %) film exhibits the best antibacterial efficacy. Phenolic compounds in the CE migrate from the film matrix into the bacterial growth medium. The eugenol groups in CE (Prasetyaningrum et al., 2021) could make CMC/PVP/CE (6 %) hydrogel more effective in destroying bacteria. Whatever its cause, this antibacterial property makes the hydrogel a stronger candidate for use in wound dressings.

Using 2,2-diphenyl-1-picrylhydrazyl (DPPH) is a simple and quick way to assess antioxidant activity. The colour changes from purple to yellow during reduction, as measured by the decreased absorbance at 517 nm. The DPPH free radical scavenging activities of the prepared samples were 25 %, 32 %, 38 %, 42 %, 48 % and 56 % for 0.1 mgL^{-1}, 0.2 mgL^{-1} 0.3 mgL^{-1}, 0.4 mgL^{-1} 0.5 mgL^{-1} and 0.6 mgL^{-1} CE solution respectively. Ascorbic acid, with the same concentration of CE, was used as a control in this investigation and the results were 30 %, 36 %, 42 %, 47 %, 54 % and 62 %, as shown in Fig. 6**c**, which were higher than CE.

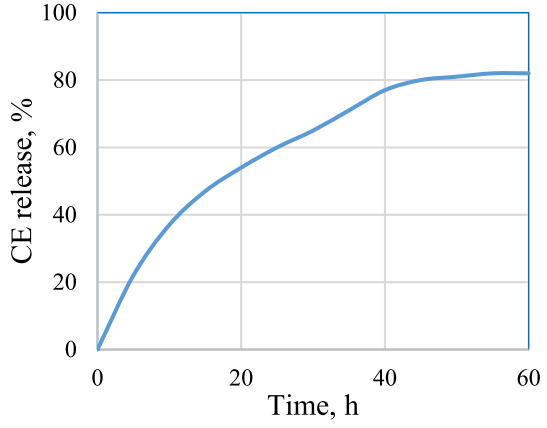

Fig. 5. CE release, % from CMC/PVP/CE (6%) bio-composite at different time intervals.

CE, with eugenol as the main bioactive compound, serves as an antioxidant by interrupting chain oxidation reactions and contributing a hydrogen atom as a free radical acceptor. This antioxidant property of the films containing CE could be attributed to phenolic compounds in CE such as eugenol, gallic acid, etc. If hydroxyl groups were attached to the aromatic ring of phenolic compounds, they could act as an electrophilic, that captures lone-paired electrons from free radicals because they are trapped in the electron cloud of the aromatic ring (Prasetyaningrum et al., 2021; González-Palma et al., 2016).

3.11. Effect of CE on cytotoxicity and blood compatability test

The cytotoxicity of CE-incorporating composite hydrogel against Vero cells was tested in an *in vitro* process. Fig. 7**a** displays the cell viability results for CMC/PVP hydrogel film containing 6 % CE, which was found to be 87.07 %. The control group, consisting of Dimethyl sulfoxide (DMSO), had a cell viability of 88.03 %, as shown in Fig. 7**b**. CE used in this study had no significant toxicity against Vero cells. So, cell viability was not significantly changed as compared to the control (Dimethyl sulfoxide solution) at the tested concentration.

Hemolytic activity rises proportionally with the increase in CE in the CMC/PVP film, reaching 2.36 % for the 6 % CE-incorporated CMC/PVP bio-composite. as indicated in Table 2. The American Society for Testing and Materials states that CE possesses moderate hemolytic characteristics. Thus, the resulting bio-composites were considered to be non-hemolytic materials.

3.12. In vivo wound healing study

Fig. 8**a** shows the results of *in vivo* wound healing experiment in albino mice. The obtained results indicated 6 % CE incorporated composite hydrogel accelerates wound healing. The CMC/PVP had 35 %, 50 %, and 70 % wound healing on days 4, 8 and 12 respectively, whereas the CMC/PVP/CE (6 %) composite hydrogel had 55 %, 76 % and 95 % wound healing for the same time periods. Nebanol antibiotic had 60 %, 80 % and 100 % wound healing for the same time periods, as shown in Fig. 8**b**. Thus we conclude that CE is an effective substance for stimulating wound healing. It is hypothesised that CE promotes keratinocyte migration to the wound site (Mittal et al. 2020).

Ion exchange may allow CMC/PVP films to absorb wound fluids. Such absorption can enhance granulation tissue production, fast epithelialisation, and healing. These processes allow wounds to heal faster. The faster wound healing with the films can be attributed to polymer degradation at the wound site, which may stimulate inflammatory cell aggregation and promote migration of epithelial, vascular endothelial, and fibroblast cells.

So, the wound healing was faster and greater when the wound was treated with CMC/PVP films than the wounds in the control (bare wound). It is worth noting that the wounds treated with CMC/PVP/CE (6 %) healed quickly through re-epithelialization with little scarring. CE, released from synthesised hydrogels plays an important role in the development of new matrices in wounds as shown in Fig. 9 (Basu et al., 2018).

4. Conclusion

PVP and CE bio-composite hydrogels, embedded with Na-CMC, were used to fabricate the new hydrogel. The hydrogels were analysed by FTIR spectroscopy, XRD, FESEM and swelling and the results confirmed the existence of CE in the bio-composite hydrogels and demonstrated

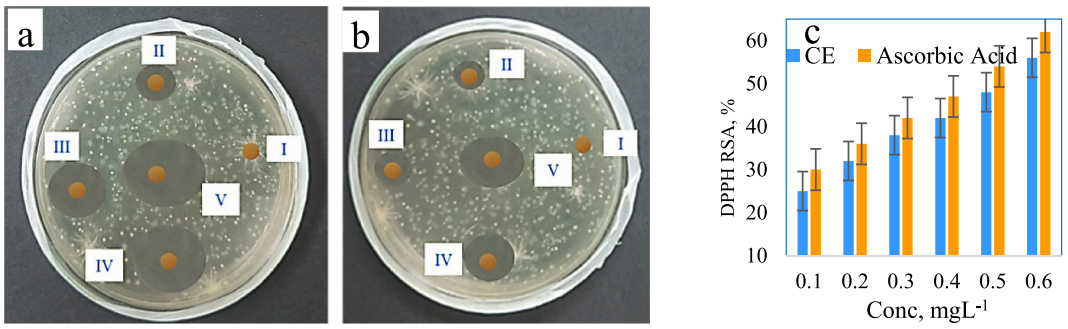

Fig. 6. (a) ZI against *S. aureus* for i. CMC/PVP, ii. CMC/PVP/CE (2%), iii. CMC/PVP/CE (4%), and iv. CMC/PVP/CE (6%), v. antibiotic; (b) ZoI against *E. coli* for i. CMC/PVP, ii. CMC/PVP/CE (2%), iii. CMC/PVP/CE (4%), and iv. CMC/PVP/CE (6%), v. antibiotic; (c) DPPH radical scavenging activity of CE and ascorbic acid (as control).

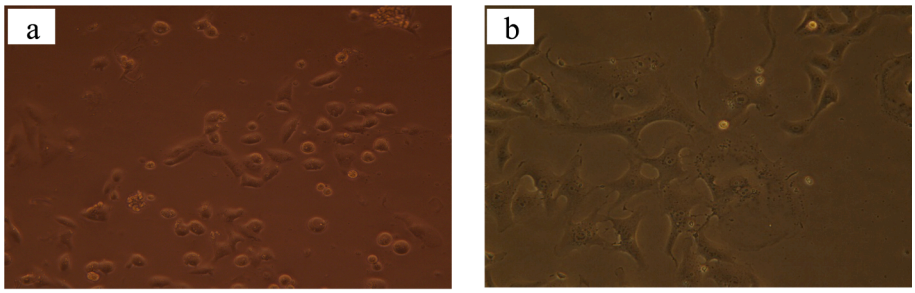

Fig. 7. (a) Effect of CE on cell viability against vero cells and (b) Effect of DMSO on cell viability against vero cells after 72 h.

Table 2
The hemolytic activity of the prepared biocomposite hydrogels.

Samples	Hemolytic activity, %
CMC/PVP	1.10 ± 0.01
CMC/PVP/CE (2 %)	1.54 ± 0.02
CMC/PVP/CE (4 %)	2.16 ± 0.01
CMC/PVP/CE (6 %)	2.36 ± 0.05

*Data are expressed as mean ± standard error of three replicates.

favourable hydrogel properties for use as a wound dressing. The ESR was highest in CMC/PVP/CE (6 %) bio-composite hydrogel at pH 7.4 is 1712 % but reduced when the CE percentage in the CMC/PVP polymer matrix reduced. CE facilitated microbial infiltration in CMC/PVP gels, which exhibited antibacterial properties against both gram-negative (*E. coli*) and gram-positive (*S. aureus*) bacteria, with greater effectiveness shown against the gram-positive *S. aureus* bacteria. The prepared bio-composite hydrogel containing 0.6 mgL^{-1} CE exhibited the greatest i.e 56 % anti-oxidant activity. An experiment using albino mice with wounds *in vitro* showed that skin wounds treated with the CMC/PVP/CE (6 %) bio-composite hydrogel healed more promptly than wounds treated with CMC/PVP hydrogel of 0 % CE. Developed bio-composite hydrogels promoted cell growth and demonstrated > 87 % cell viability when tested against Vero cells. Albino mice showed improved wound healing within 12 days and a WVTR of 2310 g/m^2-day after being treated with CMC/PVP/CE (6 %). CE extract release rates are > 80 % were observed in a bio-composite hydrogel composed of CMC, PVP, and 6 % CE. Moreover, the results of the histological analysis supported the findings of faster tissue regeneration combined with a reduction in inflammatory cells and an increase in vascularity in the surrounding skin. Overall, the

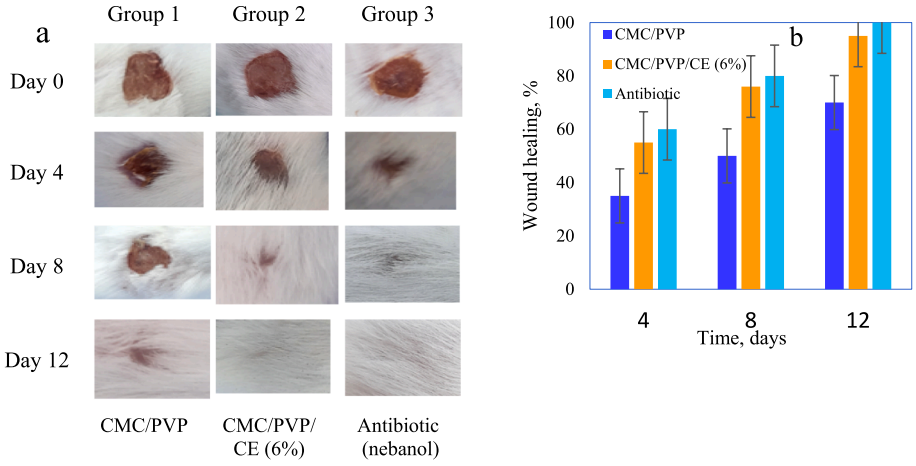

Fig. 8. **(a)** Photographs of the wounds treated with the CMC/PVP, CMC/PVP/CE (6%) biocomposite hydrogel and nebanol antibiotic at different time periods, and (b) wound healing % of CMC/PVP, CMC/ PVP/CE (6%), and nebanol antibiotic of different time intervals.

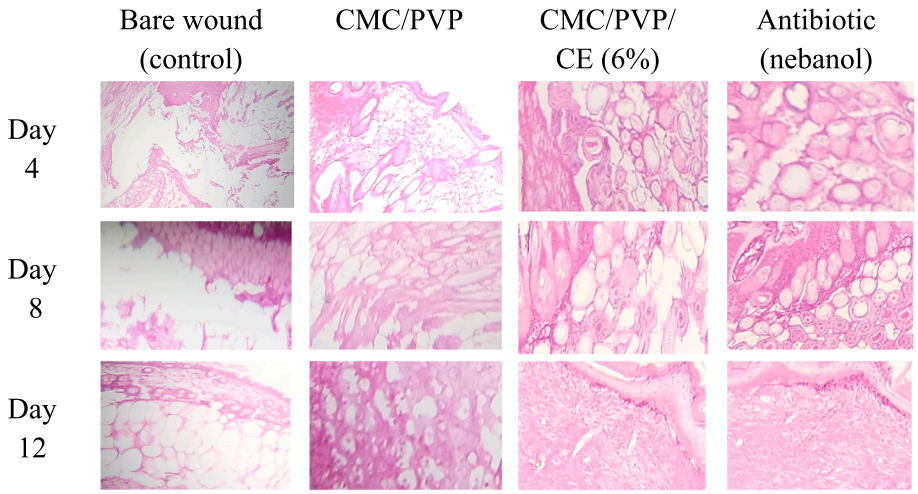

Fig. 9. H & E staining of the wound sections collected on days 4, 8 and 12 in albino mice model. Control group is untreated bare wound, and experimental group is treated with two different films (CMC/PVP, CMC/PVP/CE (6%), and antibiotic.

results support and demonstrate the wide range of possible applications for CMC/PVP/CE (6 %) bio-composite hydrogels in the biomedical sector, particularly in wound healing.

CRediT authorship contribution statement

Md. Monirul Islam: Investigation, Methodology, Formal analysis, Visualization, Writing – original draft, Writing – review & editing. **Md. Ibrahim H. Mondal:** Conceptualization, Supervision, Project administration, Resources, Funding acquisition, Formal analysis, Writing – review & editing.

Declaration of competing interest

The authors declare that they have no known competing financial interests or personal relationships that could have appeared to influence the work reported in this paper.

References

Abdollahi, Z., Zare, E.N., Salimi, F., Goudarzi, I., Tay, F.R., Makvandi, P., 2021. Bioactive carboxymethyl starch-based hydrogels decorated with CuO nanoparticles: antioxidant and antimicrobial properties and accelerated wound healing in vivo. Int. J. Mol. Sci. 22 (5), 2531. https://doi.org/10.3390/ijms22052531.

Abdul Khalil, H.P.S., Muhammad, S., Yahya, E.B., Amanda, L.K.M., Abu Bakar, S., Abdullah, C.K., Aiman, A.R., Marwan, M., Rizal, S., 2022. Synthesis and Characterization of Novel Patchouli Essential Oil Loaded Starch-Based Hydrogel. Gels 8 (9), 536. https://doi.org/10.3390/gels8090536.

Adaramola, B., Onigbinde, A., 2016. Effect of extraction solvent on the phenolic content, flavonoid content and antioxidant capacity of clove bud. IOSR J. Pharm. Biol. Sci. 11 (3), 33–38. https://doi.org/10.9790/3008-1103013338.

Ahmed, I.A.M., Babiker, E.E., Al-Juhaimi, F.Y., Bekhit, A.E.D.A., 2022. Clove polyphenolic compounds improve the microbiological status, lipid stability, and sensory attributes of beef burgers during cold storage. Antioxidants 11 (7), 1354. https://doi.org/10.3390/antiox11071354.

Alghunaim, N.S., 2019. Effect of CuO nanofiller on the spectroscopic properties, dielectric permittivity and dielectric modulus of CMC/PVP biocomposites. J. Mater. Res. Technol. 8 (4), 3596–3602. https://doi.org/10.1016/j.jmrt.2019.05.022.

Ali, A., Basit, A., Hussain, A., Sammi, S., Wali, A., Goksen, G., Muhammad, A., Faiz, F., Trif, M., Rusu, A., Manzoor, M.F., 2023. Starch-based environment friendly, edible and antimicrobial films reinforced with medicinal plants. Front. Nutr. 9, 1066337. https://doi.org/10.3389/fnut.2022.1066337.

Altaf, F., Niazi, M.B.K., Jahan, Z., Ahmad, T., Akram, M.A., Safdar, A., Butt, M.S., Noor, T., Sher, F., 2021. Synthesis and characterization of PVA/starch hydrogel membranes incorporating essential oils aimed to be used in wound dressing applications. J. Polym. Environ. 29, 156–174. https://doi.org/10.1007/s10924-020-01866-w.

Alvandi, H., Rajati, H., Naseriyeh, T., Rahmatabadi, S.S., Hosseinzadeh, L., Arkan, E., 2023. Incorporation of Aloe vera and green synthesized ZnO nanoparticles into the chitosan/PVA nanocomposite hydrogel for wound dressing application. Polym. Bull. 81 (5), 4123–4148. https://doi.org/10.1007/s00289-023-04874-7.

Anwar, M.M., Aly, S.S., Nasr, E.H., El-Sayed, E.S.R., 2022. Improving carboxymethyl cellulose edible coating using CE nanoparticles from irradiated Alternaria tenuissima. AMB Express 12 (1), 1–11. https://doi.org/10.1186/s13568-022-01459-x.

Arrua, D., Strumia, M.C., Nazareno, M.A., 2010. Immobilization of Caffeic Acid on a Polypropylene Film: Synthesis and Antioxidant Properties. J. Agric. Food Chem. 58 (16), 9228–9234. https://doi.org/10.1021/jf101651y.

Aryal, S., Baniya, M.K., Danekhu, K., Kunwar, P., Gurung, R., Koirala, N., 2019. Total phenolic content, flavonoid content and antioxidant potential of wild vegetables from Western Nepal. Plants 8 (4), 96. https://doi.org/10.3390/plants8040096.

Baghaie, S., Khorasani, M.T., Zarrabi, A., Moshtaghian, J., 2017. Wound healing properties of PVA/starch/chitosan hydrogel membranes with nano Zinc oxide as antibacterial wound dressing material. J. Biomat. Sci. Polym. Ed. 28 (18), 2220–2241. https://doi.org/10.1080/09205063.2017.1390383.

Basu, P., Narendrakumar, U., Arunachalam, R., Devi, S., Manjubala, I., 2018. Characterization and evaluation of carboxymethyl cellulose-based films for healing of full-thickness wounds in normal and diabetic rats. ACS Omega 3 (10), 12622–12632. https://doi.org/10.1021/acsomega.8b02015.

Bialik-Wąs, K., Pluta, K., Malina, D., Majka, T.M., 2021. Alginate/PVA-based hydrogel matrices with Echinacea purpurea extract as a new approach to dermal wound healing. Int. J. Polym. Mater. Polym. Biomat. 70 (3), 195–206. https://doi.org/10.1080/00914037.2019.1706510.

Blacklow, S.O., Li, J., Freedman, B.R., Zeidi, M., Chen, C., Mooney, D.J., 2019. Bioinspired mechanically active adhesive dressings to accelerate wound closure. Sci. Adva. 5 (7), eaaw3963. https://doi.org/10.1126/sciadv.aaw3963.

Chopra, H., Bibi, S., Kumar, S., Khan, M.S., Kumar, P., Singh, I., 2022. Preparation and evaluation of chitosan/PVA based hydrogel films loaded with honey for wound healing application. Gels 8 (2), 111. https://doi.org/10.3390/gels8020111.

Dai, X.Y., Nie, W., Wang, Y.C., Shen, Y., Li, Y., Gan, S.J., 2012. Electrospun emodin polyvinylpyrrolidone blended nanofibrous membrane: a novel medicated biomaterial for drug delivery and accelerated wound healing. J. Mat. Sci.: Mater. Med. 23, 2709–2716. https://doi.org/10.1007/s10856-012-4728-x.

Deng, X., Huang, B., Wang, Q., Wu, W., Coates, P., Sefat, F., Lu, C., Zhang, W., Zhang, X., 2021. A mussel-inspired antibacterial hydrogel with high cell affinity, toughness, self-healing, and recycling properties for wound healing. ACS Sustain. Chem. Eng. 9 (8), 3070–3082. https://doi.org/10.1021/acssuschemeng.0c06672.

Dharmalingam, K., Anandalakshmi, R., 2019. Fabrication, characterization and drug loading efficiency of citric acid crosslinked NaCMC-HPMC hydrogel films for wound healing drug delivery applications. Int. J. Biol. Macromol. 134, 815–829. https://doi.org/10.1016/j.ijbiomac.2019.05.027.

Edikresnha, D., Suciati, T., Munir, M.M., Khairurrijal, K., 2019. Polyvinylpyrrolidone/cellulose acetate electrospun composite nanofibres loaded by glycerine and garlic extract with in vitro antibacterial activity and release behaviour test. RSC Adv. 9 (45), 26351–26363. https://doi.org/10.1039/C9RA04072B.

El Fawal, G.F., Abu-Serie, M.M., Hassan, M.A., Elnouby, M.S., 2018. Hydroxyethyl cellulose hydrogel for wound dressing: Fabrication, characterization and in vitro evaluation. Int. J. Biol. Macromol. 111, 649–659.

El-Maati, M.F.A., Mahgoub, S.A., Labib, S.M., Al-Gaby, A.M., Ramadan, M.F., 2016. Phenolic extracts of clove (Syzygium aromaticum) with novel antioxidant and antibacterial activities. Eur. J. Integr. Med. 8 (4), 494–504. https://doi.org/10.1016/j.eujim.2016.02.006.

Farazin, A., Torkpour, Z., Dehghani, S., Mohammadi, R., Fahmy, M.D., Saber-Samandari, S., Labib, K.A., Khandan, A., 2021. A review on polymeric wound dress for the treatment of burns and diabetic wounds. Int. J. Basic Sci. Med. 6 (2), 44–50. https://doi.org/10.34172/ijbsm.2021.08.

Fiorentini, F., Suarato, G., Grisoli, P., Zych, A., Bertorelli, R., Athanassiou, A., 2021. Plant-based biocomposite films as potential antibacterial patches for skin wound

healing. Eur. Polym. J. 150, 110414 https://doi.org/10.1016/j.eurpolymj.2021.110414.
George, D., Begum, K.M.S., Maheswari, P.U., 2020. Sugarcane bagasse (SCB) based pristine cellulose hydrogel for delivery of grape pomace polyphenol drug. Waste Biomass Valori. 11, 851–860. https://doi.org/10.1007/s12649-018-0487-3.
Gholamali, I., Yadollahi, M., 2020. Doxorubicin-loaded carboxymethyl cellulose/Starch/ZnO biocomposite hydrogel beads as an anticancer drug carrier agent. Int. J. Biol. Macromol. 160, 724–735. https://doi.org/10.1016/j.ijbiomac.2020.05.232.
González-Palma, I., Escalona-Buendía, H.B., Ponce-Alquicira, E., Téllez-Téllez, M., Gupta, V.K., Díaz-Godínez, G., Soriano-Santos, J., 2016. Evaluation of the antioxidant activity of aqueous and methanol extracts of Pleurotus ostreatus in different growth stages. Front. Microbiol. 7, 1099. https://doi.org/10.3389/fmicb.2016.01099.
Gupta, B. D., Semwal, V., Pathak, A., 2020. Chapter 7-Nanotechnology-based fiber-optic chemical and biosensors. In: Thomas, S., Grohens, Y., Vignaud, G., Kalarikkal, N.., James, J., (Eds), Nano-Optics 163–195. doi: 10.1016/b978-0-12-818392-2.00007-x.
Hameed, M., Rasul, A., Waqas, M.K., Saadullah, M., Aslam, N., Abbas, G., Latif, S., Afzal, H., Inam, S., Akhtar Shah, P., 2021. Formulation and evaluation of a clove oil-encapsulated nanofiber formulation for effective wound-healing. Molecules 26 (9), 2491. https://doi.org/10.3390/molecules26092491.
Haque, M.O., Mondal, M.I.H., 2016. Synthesis and characterization of cellulose-based eco-friendly hydrogels. Rajshahi University Journal of Science and Engineering 44, 45–53.
Hosseini, S.N., Pirsa, S., Farzi, J., 2021. Biodegradable nano composite film based on modified starch-albumin/MgO; antibacterial, antioxidant and structural properties. Polym. Test. 97, 107182 https://doi.org/10.1016/j.polymertesting.2021.107182.
Huang, W.H., Hung, C.Y., Chiang, P.C., Lee, H., Lin, I.T., Lai, P.C., Chan, Y.H., Feng, S. W., 2023. Physicochemical Characterization, Biocompatibility, and Antibacterial Properties of CMC/PVA/Calendula officinalis Films for Biomedical Applications. Polymers 15 (6), 1454. https://doi.org/10.3390/polym15061454.
Jangde, R., Srivastava, S., Singh, M.R., Singh, D., 2018. In vitro and In vivo characterization of quercetin loaded multiphase hydrogel for wound healing application. Int. J. Biol. Macromol. 115, 1211–1217. https://doi.org/10.1016/j.ijbiomac.2018.05.010.
Javanbakht, S., Shaabani, A., 2019. Carboxymethyl cellulose-based oral delivery systems. Int. J. Biol. Macromol. 133, 21–29. https://doi.org/10.1016/j.ijbiomac.2019.04.079.
Karimi, A., Moradi, M.T., Hashemi, L., Alidadi, S., Soltani, A., 2017. In vitro anti-proliferative activity of clove extract on human gastric carcinoma. Res. J. Pharmacogn. 4 (4), 41–48.
Khorasani, M.T., Joorabloo, A., Moghaddam, A., Shamsi, H., MansooriMoghadam, Z., 2018. Incorporation of ZnO nanoparticles into heparinised polyvinyl alcohol/chitosan hydrogels for wound dressing application. Int. J. Biol. Macromol. 114, 1203–1215. https://doi.org/10.1016/j.ijbiomac.2018.04.010.
Kim, E.J., Choi, J.S., Kim, J.S., Choi, Y.C., Cho, Y.W., 2016. Injectable and thermosensitive soluble extracellular matrix and methylcellulose hydrogels for stem cell delivery in skin wounds. Biomacromolecules 17 (1), 4–11. https://doi.org/10.1021/acs.biomac.5b01566.
Lu, Z., Gao, J., He, Q., Wu, J., Liang, D., Yang, H., Chen, R., 2017. Enhanced antibacterial and wound healing activities of microporous chitosan-Ag/ZnO composite dressing. Carbohydr. Polym. 156, 460–469. https://doi:10.1016/j.carbpol.2016.09.051.
Mittal, A.K., Bhardwaj, R., Arora, R., Singh, A., Mukherjee, M., Rajput, S.K., 2020. Acceleration of wound healing in diabetic rats through poly dimethylaminoethyl acrylate–hyaluronic acid polymeric hydrogel impregnated with a Didymocarpus pedicellatus plant extract. ACS Omega 5 (38), 24239–24246. https://doi.org/10.1021/acsomega.0c02040.
Mohammadi, H., Kamkar, A., Misaghi, A., 2018. Biocomposite films based on CMC, okra mucilage and ZnO nanoparticles: Physico mechanical and antibacterial properties. Carbohydr. Polym. 181, 351–357. https://doi.org/10.1016/j.carbpol.2017.10.045.
Mondal, M.I.H., Haque, M.O. (2019). Cellulosic Hydrogels: A Greener Solution of Sustainability. In: Mondal, M. (eds), Cellulose-Based Superabsorbent Hydrogels, Springer, Switzerland, pp. 3-35. doi: 10.1007/978-3-319-77830-3_4.
Mondal, M.I.H., Haque, M.O., Ahmed, F., Pervez, M.N., Naddeo, V., Ahmed, M.B., 2022. Super-Adsorptive biodegradable hydrogel from simply treated sugarcane bagasse. Gels 8 (3), 177. https://doi.org/10.3390/gels8030177.
Mondal, M.I.H., Saha, J., 2019. Antimicrobial, UV resistant and thermal comfort properties of chitosan-and Aloe vera-modified cotton woven fabric. J. Polym. Environ. 27, 405–420. https://doi.org/10.1007/s10924-018-1354-9.
Mondal, M.I.H., Yeasmin, M.S., Rahman, M.S., 2015. Preparation of food grade carboxymethyl cellulose from corn husk agrowaste. Int. J. Biol. Macromol. 79, 144–150. https://doi.org/10.1016/j.ijbiomac.2015.04.061.
Parthipan, P., AlSalhi, M.S., Devanesan, S., Rajasekar, A., 2021. Evaluation of Syzygium aromaticum aqueous extract as an eco-friendly inhibitor for microbiologically influenced corrosion of carbon steel in oil reservoir environment. Bioprocess Biosyst. Eng. 44, 1441–1452. https://doi.org/10.1007/s00449-021-02524-8.
Pornpitchanarong, C., Rojanarata, T., Opanasopit, P., Ngawhirunpat, T., Bradley, M., Patrojanasophon, P., 2022. Maleimide-functionalized carboxymethyl cellulose: A novel mucoadhesive polymer for transmucosal drug delivery. Carbohydr/ Polym. 288, 119368 https://doi.org/10.1016/j.carbpol.2022.119368.
Pourjavadi, A., Barzegar, S., Mahdavinia, G.R., 2006. MBAcrosslinked Na-Alg/CMC as a smart full-polysaccharide superabsorbent hydrogels. Carbohydr. Polym. 66 (3), 386–395. https://doi.org/10.1016/j.carbpol.2006.03.013.
Pramod, K., Ilyas, U.K., Kamal, Y.T., Ahmad, S., Ansari, S.H., Ali, J., 2013. Development and validation of RP-HPLC-PDA method for the quantification of eugenol in developed nanoemulsion gel and nanoparticles. J. Ana. Sci. Technol. 4, 1–6. https://doi.org/10.1186/2093-3371-4-16.
Pramod, K., Suneesh, C.V., Shanavas, S., Ansari, S.H., Ali, J., 2015. Unveiling the compatibility of eugenol with formulation excipients by systematic drug-excipient compatibility studies. J. Analyt. Sci. Technol. 6 (1), 1–14. https://doi.org/10.1186/s40543-015-0073-2.
Prasetyaningrum, A., Utomo, D.P., Raemas, A.F.A., Kusworo, T.D., Jos, B., Djaeni, M., 2021. Alginate/κ-carrageenan-based edible films incorporated with clove essential oil: physico-chemical characterization and antioxidant-antimicrobial activity. Polymers 13 (3), 354. https://doi.org/10.3390/polym13030354.
Qamruzzaman, M., Ahmed, F., Mondal, M.I.H., 2022. An overview on starch-based sustainable hydrogels: Potential applications and aspects. J. Polym. Environ. 30 (1), 19–50. https://doi.org/10.1007/s10924-021-02180-9.
Ramadoss, P., Regi, T., Rahman, M.I., Arivuoli, D., 2019. Low-cost and biodegradable cellulose/PVP/activated carbon composite membrane for brackish water treatment. J. Appl. Polym. Sci. 137 (22), 48746. https://doi.org/10.1002/app.48746.
Rashid, N., Khalid, S.H., Ullah Khan, I., Chauhdary, Z., Mahmood, H., Saleem, A., Umair, M., Asghar, S., 2023. Curcumin-Loaded Bioactive Polymer Composite Film of PVA/Gelatin/Tannic Acid Downregulates the Pro-inflammatory Cytokines to Expedite Healing of Full-Thickness Wounds. ACS Omega 8 (8), 7575–7586. https://doi.org/10.1021/acsomega.2c07018.
Roy, N., Saha, N., Kitano, T., Saha, P., 2012. Biodegradation of PVP–CMC hydrogel film: A useful food packaging material. Carbohydr. Polym. 89 (2), 346–353. https://doi.org/10.1016/j.carbpol.2012.03.008.
Saha, J., Mondal, M.I.H., Ahmed, F., Rahman, M., 2023. Extraction, characterization and functionality assessment of Aloe vera, chitosan and silk sericin. Arab. J. Chem. 16 (9), 105087 https://doi.org/10.1016/j.arabjc.2023.105087.
Saha, N., Saarai, A., Roy, N., Kitano, T., Saha, P., 2011. Polymeric Biomaterial Based Hydrogels for Biomedical Applications. J. Biomater. Nanobiotechnol. 02 (01), 85–90. https://doi.org/10.4236/jbnb.2011.21011.
Sriyanti, I., Marlina, L., Fudholi, A., Marsela, S., Jauhari, J., 2021. Physicochemical properties and In vitro evaluation studies of polyvinylpyrrolidone/cellulose acetate composite nanofibres loaded with Chromolaena odorata (L) King extract. J. Mater. Res. Technol. 12, 333–342. https://doi.org/10.1016/j.jmrt.2021.02.083.
Stanicka, K., Dobrucka, R., Woźniak, M., Sip, A., Majka, J., Kozak, W., Ratajczak, I., 2021. The effect of chitosan type on biological and physicochemical properties of films with propolis extract. Polymers 13 (22), 3888. https://doi.org/10.3390/polym13223888.
Taokaew, S., Seetabhawang, S., Siripong, P., Phisalaphong, M., 2013. Biosynthesis and Characterization of Nanocellulose-Gelatin Films. Materials 6 (3), 782–794. https://doi.org/10.3390/ma6030782.
Tayel, A.A., Elzahy, A.F., Moussa, S.H., Al-Saggaf, M.S., Diab, A.M., 2020. Biopreservation of shrimps using composed edible coatings from chitosan nanoparticles and cloves extract. J. Food Qual. Article ID 8878452, (10 pages). https://doi.org/10.1155/2020/8878452.
Wang, J., Hao, S., Luo, T., Cheng, Z., Li, W., Gao, F., Guo, T., Gong, Y., Wang, B., 2017. Feather keratin hydrogel for wound repair: preparation, healing effect and biocompatibility evaluation. Colloids Surf. b: Biointerfaces 149, 341–350. https://doi.org/10.1016/j.colsurfb.2016.10.038.
Wang, T., Liao, Q., Wu, Y., Wang, X., Fu, C., Geng, F., Qu, Y., Zhang, J., 2020. A composite hydrogel loading natural polysaccharides derived from Periplaneta americana herbal residue for diabetic wound healing. Int. J. Biol. Macromol. 164, 3846–3857. https://doi.org/10.1016/j.ijbiomac.2020.08.156.
Wang, M., Xu, L., Hu, H., Zhai, M., Peng, J., Nho, Y., Lia, J., Wei, G., 2007. Radiation synthesis of PVP/CMC hydrogels as wound dressing. Nucl. Instrum. Methods Phys. Res., Sect. B 265 (1), 385–389. https://doi.org/10.1016/j.nimb.2007.09.009.
Yeasmin, M.S., Mondal, M.I.H., 2015. Synthesis of highly substituted carboxymethyl cellulose depending on cellulose particle size. Int. J. Biol. Macromol. 80, 725–731. https://doi.org/10.1016/j.ijbiomac.2015.07.040.
Yuan, F.Z., Wang, H.F., Guan, J., Fu, J.N., Yang, M., Zhang, J.Y., Chen, Y.R., Wang, X., Yu, J.K., 2021. Fabrication of injectable chitosan-chondroitin sulfate hydrogel embedding kartogenin-loaded microspheres as an ultrasound-triggered drug delivery system for cartilage tissue engineering. Pharmaceutics 13 (9), 1487. https://doi.org/10.3390/pharmaceutics13091487.
Zamora-Mendoza, L., Vispo, S.N., De Lima, L., Mora, J.R., Machado, A., Alexis, F., 2023. Hydrogel for the controlled delivery of bioactive components from extracts of eupatorium glutinosum lam. Leaves. Molecules 28 (4), 1591. https://doi.org/10.3390/molecules28041591.